Polymer Testing
Volume 96, April 2021, 107093

PVDF-HFP/NKBT composite dielectrics: Perovskite particles induce the appearance of an additional dielectric relaxation process in ferroelectric polymer matrix

Vera P. Pavlović [a], Dragana Tošić [b], Radovan Dojčilović [b], Duško Dudić [b], Miroslav D. Dramićanin [b], Mina Medić [b], Michael M. McPherson [c], Vladimir B. Pavlović [d, e], Branislav Vlahovic [f, g] ✉, Vladimir Djoković [b] ✉

[a] University of Belgrade, Faculty of Mechanical Engineering, Kraljice Marije 16, 11120, Belgrade, Serbia
[b] Vinča Institute of Nuclear Sciences, National Institute of the Republic of Serbia, University of Belgrade, P.O. Box 522, 11001, Belgrade, Serbia
[c] Cape Peninsula University of Technology, P.O. Box 652, Cape Town 8000, South Africa
[d] University of Belgrade, Faculty of Agriculture, Nemanjina 6, 11080 Belgrade, Serbia
[e] Institute of Technical Sciences, SASA, Knez Mihailova 35/IV 11000, Belgrade, Serbia
[f] North Carolina Central University, Durham, NC, 27707, USA
[g] NASA University Research Center for Aerospace Device Research and Education and NSF Center of Research Excellence in Science and Technology Computational Center for Fundamental and Applied Science and Education, Durham, NC, 27707, USA

Received 13 July 2020, Revised 22 December 2020, Accepted 26 January 2021, Available online 29 January 2021, Version of Record 13 February 2021.

https://doi.org/10.1016/j.polymertesting.2021.107093

Highlights

- $Na_{0.25}K_{0.25}Bi_{0.5}TiO_3$ (NKBT) perovskite particles are synthesized by solid state method.
- PVDF-HFP/NKBT composite films were prepared by solution mixing.
- NKBT particles induce an increase in effective dielectric permittivity of the films.
- An additional transition peak was observed in the dielectric spectra of the composite film.
- The magnitude of the novel transition depends on the NKBT content.

Abstract

$Na_{0.25}K_{0.25}Bi_{0.5}TiO_3$ (NKBT) perovskite particles are synthesized by solid-state method and used as a filler for polyvinylidene fluoride-co-hexafluoropropylene (PVDF-HFP) co-polymer. X-ray diffraction analysis of NKBT powders shows that the particles have a rhombohedral perovskite crystal structure (R3c symmetry). Raman spectroscopy reveals that the co-polymer crystallizes predominantly into the mixture of polar β- and γ-crystals, while there is also a contribution of the non-polar α-crystal phase. The introduction of the NKBT into the PVDF-HFP results with an increase in effective dielectric permittivity and this effect depends on the inorganic content in the composite. The most interesting result of the present study is that the introduction of NKBT particles induces the appearance of an additional transition peak in the dielectric spectra of the co-polymer matrix. At the fixed frequency of ~2 kHz, the observed process appears at ~10 °C (about 45° above the glass transition temperature) and its magnitude strongly depends on the amount of the NKBT in the composite. Dielectric spectroscopy measurements of the composites are carried out in the wide range of frequencies (from 0.1 Hz to 1 MHz) and temperatures (from –100 to 100 °C). They reveal that the novel process can be clearly distinguished in the frequency range between 160 Hz and ~50 kHz.

Previous Next

Keywords

Dielectric relaxation spectroscopy; PVDF-HFP; Composite; Perovskite; NKBT

Abbreviations

DSC, Differential scanning calorimetry; DMF, dimethylformamide; NKBT, Na0.25K0.25Bi0.5TiO3; PVDF, polyvinylidene fluoride; PVDF-HFP, polyvinylidene fluoride-co-hexafluoropropylene; PVDF-TrFE, polyvinylidene fluoride-co-trifluorethylene; PZT, PbZrxTi1-xO3; SEM, Scanning electron microscopy; VTF, Vogel-Tammann-Fulche; XRD, X-ray diffraction

1. Introduction

The design and development of novel piezoelectric polymer-ceramic composites for specific applications are the subjects of intensive research [[1], [2], [3], [4]]. In these heterostructural materials, the excellent dielectric properties of ceramics are combined with beneficial properties of polymers such as easy processing, high breakdown strength and flexibility. The resulting composite material may also exhibit additional synergetic properties that are not present in either of the single-phase materials observed separately. Typically, PZT ($PbZr_xTi_{1-x}O_3$), $BaTiO_3$, ZnO and TiO_2 were used as fillers for ferroelectric polymers such as polyvinylidene fluoride (PVDF) and its copolymers with trifluorethylene (PVDF-TrFE) and hexafluoropropylene (PVDF-HFP) [[1], [2], [3], [4], [5], [6], [7], [8], [9], [10], [11], [12], [13], [14], [15], [16], [17], [18], [19], [20]]. Recent studies involved various other high dielectric constant particles such as $SrTiO_3$, $CaTiO_3$, $Ba_{0.5}Sr_{0.5}TiO_3$, K_2CO_3, $K_xTi_yNi_{1-x-y}O$, as an inorganic phase in PVDF based composites [[21], [22], [23], [24], [25]]. Taking into account current trends towards replacing Pb-based with environmentally more benign piezoelectric ceramics, we decide to use $Na_{0.25}K_{0.25}Bi_{0.5}TiO_3$ (NKBT) as filler for PVDF-HFP copolymer and to investigate the dielectric properties of the obtained composites.

$Na_{0.5}Bi_{0.5}TiO_3$ (NBT) is a lead-free ferroelectric material extensively studied due to favourable properties such as high Curie temperature (T_c ~320 °C) coupled with a large remnant polarization and a large piezoelectric strain constant (d_{33}) [26]. On the other hand, relatively high coercive field (E_c) and high conductivity are the drawbacks for its wide-spread applications [27]. It

was shown that the introduction of a certain amount of potassium under specific processing conditions can improve the remnant polarization and lower the coercive field [[28], [29], [30], [31], [32], [33]]. In the present study, $Na_{0.25}K_{0.25}Bi_{0.5}TiO_3$ (NKBT) ceramics were synthesized by solid-state reaction. The obtained NKBT powder was solution mixed with PVDF-HFP and the obtained composite films were investigated by means of the dielectric spectroscopy in the temperature range from –100 to 100 °C at various frequencies. It was found that the introduction of the ceramic particles induces the appearance of the additional relaxation peak in the spectra of the composite, which is not present in the pure co-polymer. From the fundamental point of view, this was an interesting result and the study is focused on the properties of the observed relaxation transition. The intensity of the relaxation peak strongly depends on the amount of the inorganic particles in the matrix. Also, the transition is dependent on the frequency of the external field and starts to disappear as a separate peak at the frequencies above 100 kHz.

2. Experimental

2.1. Materials

Polyvinylidene fluoride-co-hexafluoropropylene (Mw~455000 and Mñ110000) and the precursor materials for the preparation of NKBT (TiO_2, Bi_2O_3, Na_2CO_3 and K_2CO_3) were purchased from Aldrich.

$Na_{0.25}K_{0.25}Bi_{0.5}TiO_3$ (NKBT) powder was fabricated via solid-state reaction of the precursors. TiO_2, Bi_2O_3, Na_2CO_3 and K_2CO_3 powders were ball milled in ethanol for 12 h, dried and calcinated at 850 °C for 2 h. After that, the obtained powders were additionally milled in ethanol for 12 h and finally sintered at 850 °C for 4 h.

PVDF-HFP/NKBT composites were prepared by solution mixing at room temeprature. PVDF-HFP solution (2 wt%) was prepared by dissolving 3 g of polymer in 150 ml dimethylformamide (DMF). NKBT powders were dispersed in 50 ml DMF and sonicated in a BransonW-450 D Digital Sonifier for 20 min at 80 W amplitude. The obtained dispersion was mixed in specific ratios with the co-polymer solution in order to obtain the composites with 2.5, 5, and 10 wt% of inorganic content. The pristine polymer and composite films (~80 μm thick) were prepared by casting the mixtures into Petri dishes. The films were first dried at room temeperature (20 °C) for 24 h and then in the oven at 90 °C for 1 h.

2.2. Methods

Morphology of NKBT powders, PVDF-HFP co-polymer and PVDF-HFP/NKBT nanocomposite films were investigated by a field emission gun TESCAN MIRA3 scanning electron microscope. For SEM (Scanning electron microscopy) analyses, the films were fractured after immersion in liquid nitrogen. The samples were covered with gold by sputtering (Polaron SC502 - Fison Instruments, UK) and investigated at 3.5 kV (films) and 20 kV (powder).

X-ray diffraction (XRD) measurements were carried out on a Rigaku SmartLab diffractometer using Cu-Ka radiation (λ = 0.15405 nm). Diffraction patterns were recorded with a step size of 0.02° over the 2θ angular range from 10° to 120°.

Diffuse reflection spectra measurements were recorded with 1 nm resolution on a Shimadzu UV–Visible UV-2600 (Shimadzu Corporation, Japan) spectrophotometer equipped with an integrated sphere [ISR-2600 Plus (for UV-2600)] in the range from 220 nm to 1300 nm. Teflon was used as a reflectance standard.

Raman spectroscopy measurements of the composite films were performed on a Horiba Jobin Yvon Lab Ram ARAMIS Raman microscope. The samples were excited by using the He–Ne laser at 633 nm (1 mW at the sample) and the data were collected in a Raman shift range from 100 to 1500 cm^{-1} by using a 100 × objective. The acquisition time was 10 s with 5 averaging cycles.

Dielectric spectra of the pure co-polymer and the composite films were acquired over a broad frequency (10–10^6 Hz) and temperature (100–110 °C) ranges using a Hewlett Packard 4284A LCR meter in conjunction with a Delta Design oven model 2300. Heating rate was 5 °Cmin^{-1}. Gold electrodes with an average thickness of 60 nm were sputtered on both sides of the films for the electrical measurements.

Differential scanning calorimetry measurements were performed on a Setaram DSC 151R thermal analyzer in the nitrogen atmosphere. The samples were heated from 25 to 160 °C at 10 $Cmin^{-1}$.

3. Results and discussion

3.1. Morphology and structure

SEM micrographs of the NKBT powder, pure PVDF-HFP co-polymer and PVDF-HFP/NKBT composite (with 10 wt% of inorganic content) are shown in Fig. 1a,b,c. SEM image of the powder in Fig. 1a shows the agglomerated ceramic particles with a diameter of ~100 nm. It can also be seen that the fracture surface of the pure PVDF-HFP film is relatively smooth (Fig. 1b). SEM image of PVDF-HFP/NKBT composite (Fig. 1c) reveals that the particles are well dispersed in the matrix.

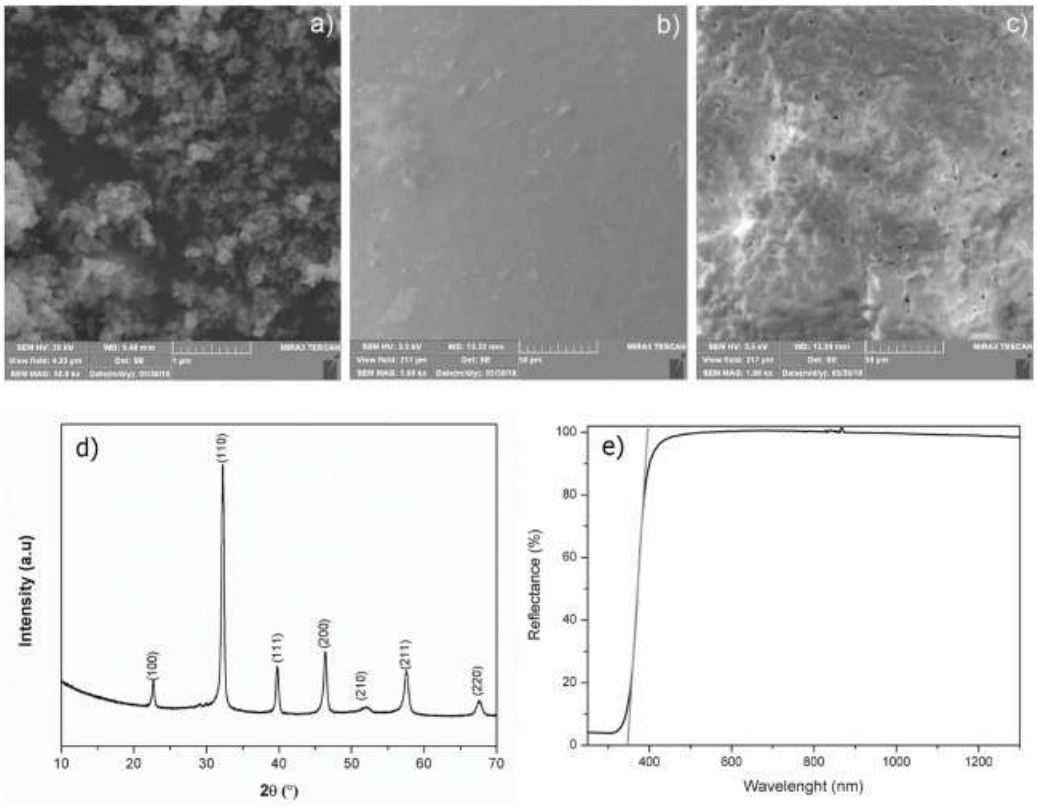

Download : Download high-res image (1MB)

Download : Download full-size image

Fig. 1. SEM micrographs of a) NKBT powder, b) pure PVDF-HFP co-polymer, c) PVDF HFP/NKBT composite (10 wt% of NKBT) films; d) X-ray diffraction pattern of the NKBT powder; e) Diffuse reflectance spectrum of the NKBT ceramic.

Fig. 1d shows the XRD pattern of NKBT powder. The observed (100), (110), (111), (200), (210), (112) (220) peaks correspond to the rhombohedral perovskite crystal structure of NKBT with R3c symmetry [[29], [30], [31], [32]]. The tetragonal phase, which is sometimes present in NKBT system, was not observed, since there was no splitting of the peak related to the (200) reflection.

The diffuse reflectance spectrum of the NKBT sample is shown in Fig. 1e. A high reflectance of 99% was observed in the wide range of wavelengths from 450 to 1200 nm. The linear part of the reflectance curve prior to plateau value provides information about the onset of the optical absorption. The linear fit (the straight line in Fig. 1e) intersects the x-axis at 345 nm, which corresponds to the value of energy bandgap of 3.6 eV. The result is in agreement with literature data [34,35], that report NKBT as a semiconductor with the direct optical bandgap of 3.6 eV.

Fig. 2 shows the Raman spectra of the pure PVDF-HFP co-polymer and PVDF-HFP/NKBT composites (with 2.5, 5, and 10 wt% of inorganic content). The Raman spectrum of the pure co-polymer suggests that the film contains the mixture of typical crystal phases of PVDF i.e. α, β and γ. The analysis of the Raman shift region from 780 to 900 cm^{-1} revealed that the crystallization of the co-polymer is directed towards the formation of polar, β and γ, crystals. This crystallization behavior is typical for the PVDF based co- and ter-polymers [36] and it is confirmed by the appearance of the pronounced Raman peaks at ~837 cm^{-1} (attributed to very strong Raman modes of β and γ crystal phases) and at ~810 cm^{-1} (attributed to very strong mode of γ phase) [36,37]. It can also be seen that the Raman peak at the ~800 cm^{-1}, which corresponds to the strongest line in the spectra of the pure α-crystal phase, is present as a shoulder in the spectrum of PVDF-HFP. A comparison of the spectra in Fig. 2 implies also that the introduction of the filler particles promotes the crystallization of the γ-phase. As the concentration of the filler increases, an increase in the intensity of the peak at ~1130 cm^{-1} was observed, which is attributed to the enhancement of C–C and/or $–CF_2$ stretching vibrations [38,39].

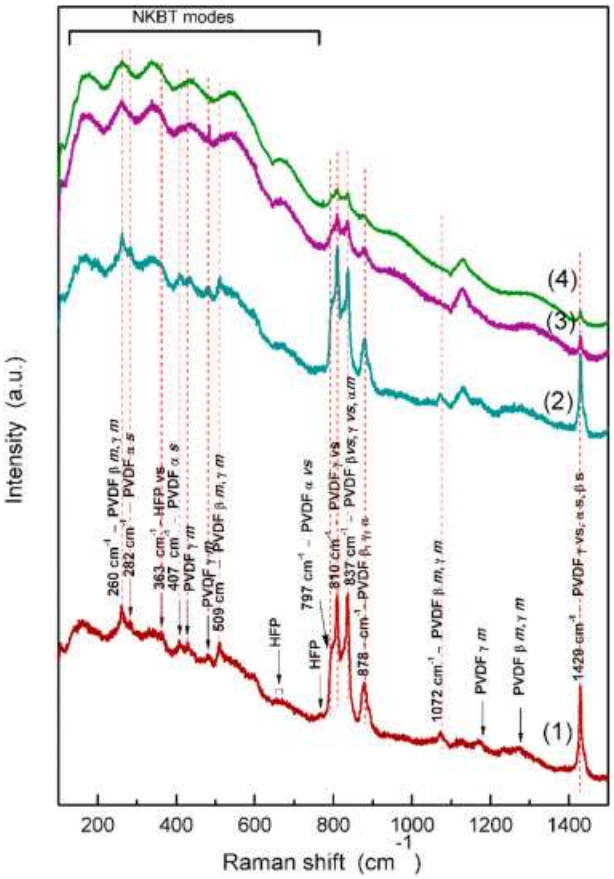

Download : Download high-res image (667KB) Download : Download full-size image

Fig. 2. Raman spectra of 1) pure PVDF-HFP co polymer and PVDF-HFP/NKBT composites with 2) 2.5 wt%, 3) 5 wt% and 4) 10 wt% of inorganic content.

In the spectra of the composites with a higher percentage of the filler, one can also notice a decrease in the intensities of the peaks in the 780-900 cm^{-1} range. This might be a consequence of reduced thickness of the crystals. On the other hand, the Raman peaks in the range below 750 cm^{-1} become more pronounced. The observed increase in the intensity of the peaks originates probably from the contribution of the broad Raman peaks of the NKBT filler, which generally appear in that part of the spectrum and originate from the convolution of a large number of the Raman modes [33]. A disorder in the A position of the perovskite might additionally contribute to the widening of the Raman peaks [33].

DSC endotherms of the pure PVDF-HFP co-polymer and its composites with NKBT are shown in Fig. 3.

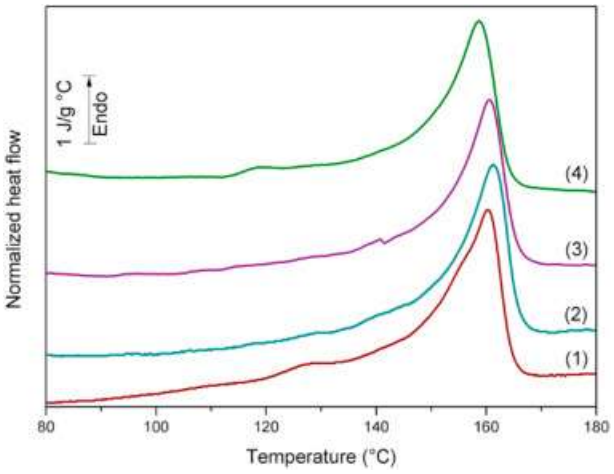

Download : Download high-res image (240KB) Download : Download full-size image

Fig. 3. DSC melting curves of 1) pure PVDF-HFP co polymer and PVDF-HFP/NKBT composites with 2) 2.5 wt%, 3) 5 wt% and 4) 10 wt% of inorganic content.

DSC results suggest that the overall crystallinity of the matrix is not significantly affected by the presence of filler. On the other hand, there is a shift of the melting peak towards the lower temperatures with an increase in inorganic content. This implies that the introduction of the inorganic particles reduces the thickness of the crystals in the host matrix.

3.2. Electrical properties

Fig. 4 shows dielectric constant (ε') and dielectric loss (ε'') curves of the pure PVDF-HFP co-polymer and its composites as a function of frequency at a constant temperature of 20 °C. It can be seen that the composites have higher values of dielectric constant than the pure matrix (at fixed temperature and frequency).

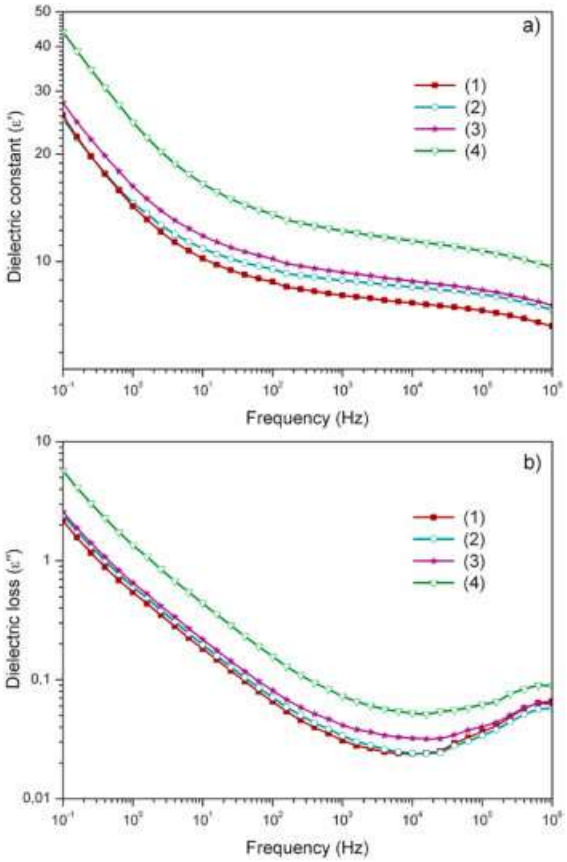

Download : Download high-res image (398KB) Download : Download full-size image

Fig. 4. a) Dielectric constant and b) dielectric loss vs. frequency for the pure (1) PVDF-HFP copolymer and PVDF-HFP/NKBT composites with (2) 2.5, (3) 5, (4) 10 wt% of filler. The legend is given.

All four materials show similar dependence of dielectric constant on frequency i.e. dielectric constant increases with decreasing in frequency from 10^6 to 10^{-1} Hz. An increase in ε' is especially pronounced in the region of low frequencies (0.1–10 Hz) due to polarization effects. In the case of composite materials, the both components contribute to the effective dielectric constant of the composite. However, the polymer matrix contributes more to the effective dielectric permittivity, due to the much higher dielectric permittivity of perovskite particles [19]. Typically, to increase the permittivity of the composite, one needs a higher concentration of the filler. For this reason, we consider that an increase in effective dielectric constant of the composite (Fig. 4a) originates from the synergetic effects of a high dielectric constant of NKBT particles and reduced mobility of the chains after their introduction into copolymer matrix. Dielectric loss vs. frequency curves of the PVDF-HFP co-polymer and the PVDF-HFP/NKBT composites obtained at room temperature are shown in Fig. 4b.

As can be seen, the dielectric losses are high at low frequencies (0.1–10 Hz) due to polarization effects and decrease with increasing frequency (up to 10^4 Hz). At frequencies above 10^4 Hz another process is observed in ε'' curves, which is usually associated with dipole relaxations [20].

It should be noted that the dielectric relaxation measurements as a function of frequency were performed at different temperatures (in the range from –100 to 100 °C). In the main text, we decided to present the most interesting dielectric spectra. The complete sets of the results were included in the Supporting information and the figures were referred in the discussion as S1, S2, etc. The $\varepsilon'(f)$ and $\varepsilon''(f)$ curves of the pure PVDF-HFP and its composite with 10 wt% of NKBT filler at various temperatures are shown in Figs. S1 and S2, respectively. Dielectric spectra of the pressed tablet of NKBT powder are also included (Fig. S3). In the low-frequency/high-temperature intervals, dielectric loss curves of PVDF-HFP and PVDF-HFP/NKBT composite (Figs. S1b and S2b) show the linear dependence on frequency, which is typical for conductivity

relaxations [40]. In the lowest-frequency/highest-temperature intervals the frequency dependences of ε'' deviates slightly from the linear behavior, which is attributed to the accumulation of charges at the electrode-sample interfaces [41]. In order to study the mechanism of conduction, in Fig. 5, the specific conductivities (σ_{AC}) curves of the pure PVDF-HFP and PVDF-HFP/NKBT composite (with 10 wt% of filler) at fixed temperatures (t > 70 °C) were given as a function of frequency. At low frequencies, the specific conductivities have constant values and the plateaus in σ_{AC} curves in Fig. 5 correspond to the DC conductivities (σ_{DC}).

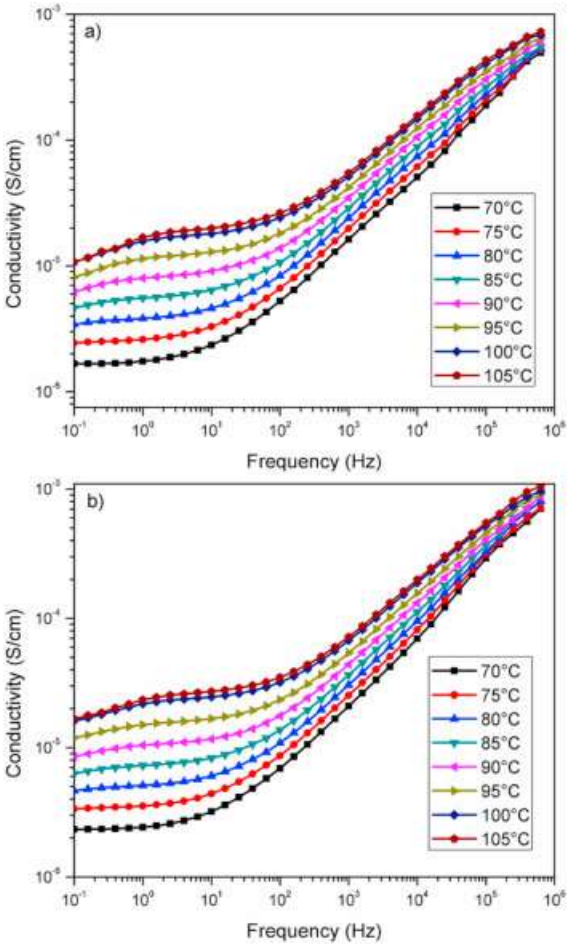

Download : Download high-res image (611KB) Download : Download full-size image

Fig. 5. Conductivity (σ_{AC}) vs. frequency curves at various temperatures for the a) pure PVDF-HFP copolymer and b) PVDF HFP/NKBT composite with 10 wt% of filler.

The dependence of the obtained σ_{DC} values from inverse temperature can be described by empirical Vogel-Tammann-Fulche (VTF) equation

$$\sigma_{DC} = \sigma_{DC0}\exp\left[-\frac{B}{T-T_0}\right] \quad (1)$$

where σ_{DC0}, B and T_0 are fitting parameters [42].

In Fig. 6, $\log\sigma_{DC}$ values of the neat PVDF-HFP and PVDF-HFP/NKBT composites were plotted against 1/T and fitted to equation (1). It should be noticed that the composites with lower concentration of NKBT filler (2.5 and 5 wt%) has lower DC conductivity values than that of the neat copolymer. At the highest concentration of the filler (10 wt%), DC conductivity values of the composite exceeds the conductivity of pure matrix probably due to decrease in the average distances between the particles. According to Lewis's model, there is accumulation of the charges at the particles surfaces due to differences in

Fermi levels or chemical potentials of the particles and the host polymer [1,43]. This, in turn, results in formation of counter charge in the polymer chains at the interface layers. Eventually, due to Coulomb interaction, the charged particles form electrical double layer that consists of a Stern layer and a Gouy–Chapman diffused layer [43]. Diffused layer contains trapped positive and negative ions and it significantly affects the dielectric properties of the composite [44]. Conduction via diffuse layers becomes increasingly important at higher filler concentrations and near the percolation threshold, as the particles get closer together. It can also be seen that the VTF equation describes well the dependence of $\log\sigma_{DC}$ from inverse temperature, which suggests that the conductivity of the films in low frequency/high-temperature ranges is controlled by the segmental mobility of chains [41].

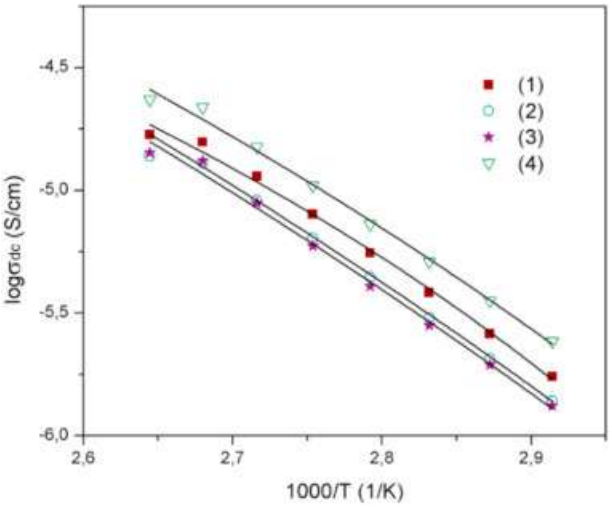

Download : Download high-res image (197KB) Download : Download full-size image

Fig. 6. Dependence of log σ_{dc} on reciprocal temperature for (1) PVDF-HFP copolymer and PVDF-HFP/NKBT composites with (2) 2.5, (3) 5, (4) 10 wt% of filler. Solid lines are fits of Eq. (1) to the experimental data.

Of course, this effect is far less important at low temperatures, while below the glass transition temperature, when segmental mobility is reduced, the dependences $\log\sigma_{DC}$ from 1/T becomes linear [40]. The VTF parameters obtained by fitting the experimental data to Eq. (1) are presented in Table 1.

Table 1. Parameters obtained by fitting Eq. (1) to experimental log σ_{dc} (1/T) curves in Fig. 8.

Sample	log σ_{dc} (S/m)	T_0(K)	B
PVDF-HFP/NKBT 0 wt%	–2.01	251.51	794.40
PVDF-HFP/NKBT 2.5 wt%	–1.82	243.56	929.75
PVDF-HFP/NKBT 5 wt%	–1.80	245.79	921.36
PVDF-HFP/NKBT 10 wt%	–0.53	206.20	1608.67

Fig. 7 shows dielectric spectra (ε' and ε'') as function of temperature at fixed frequency of ~2 kHz. As can be seen, ε' of PVDF-HFP and PVDF-HFP/NKBT composites increases with temperature, which is typical dielectric behaviour of ferroelectric polymers at constant frequency of external field (Fig. 7a) [[45], [46], [47]].

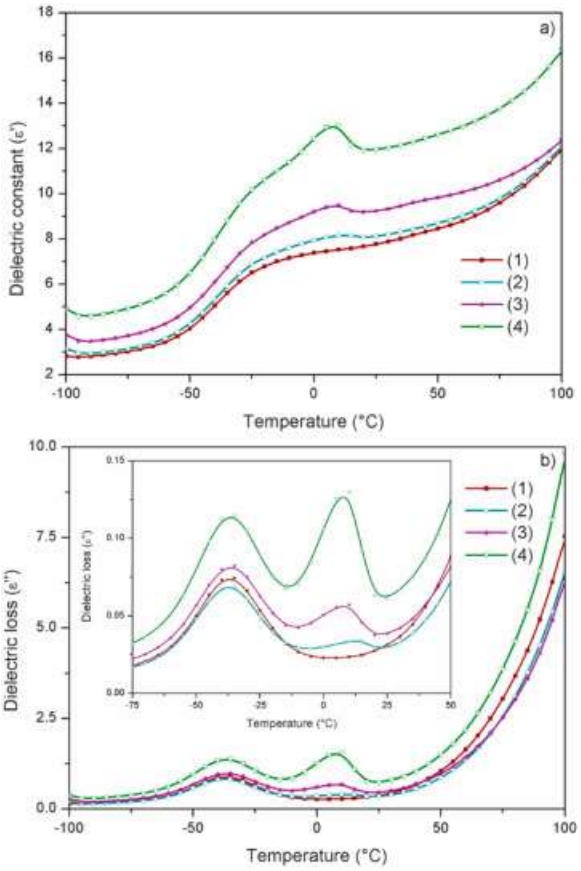

Download : Download high-res image (450KB) Download : Download full-size image

Fig. 7. a) Dielectric constant and b) dielectric loss vs. temperature for the pure (1) PVDF-HFP copolymer and PVDF-HFP/NKBT composites with (2) 2.5, (3) 5, (4) 10 wt% of filler. In the inset of Fig. 7, dielectric loss curves are presented in the range from –75 to 50 °C in order to emphasize the appearance of the additional relaxation peak at ~10 °C in the spectra of composites.

An increase in dielectric constant with an increase in temperature is a consequence of activation of the molecular dipoles i.e. the dipole segments, which are frozen in glassy state start to contribute to dielectric spectra after the transition of the material into the rubbery state. Model suggested by Tanaka assumes that introduction of spherical particles into polymer matrix is followed by formation of a specific interface layer at the boundary of the phases [43]. This interface layer consists of bonded layer (~1 nm), bound layer (2–9 nm) and loose layer (several tens of nm). The mobility and conformation of the chains as well as the crystallinity and free volume of the polymer in these regions are different then in the bulk matrix [43]. Due to changes in distribution and orientation of the dipoles in the interfacial layers, the broad dielectric constant peak of the co-polymer becomes more pronounced as filler content increases (Fig. 7a).

Dielectric loss spectra of PVDF-HFP and its composites exhibit peak at –35 °C, which corresponds to the glass transition (Fig. 7b) [[45], [46], [47]]. The position of the glass transition peak is not significantly affected by the presence of the filler. On the other hand, in the loss spectra of the composites, one can also notice the additional peak positioned at ~10 °C. This process is also a result of the changes in packing density of the matrix chains in the vicinities of the NKBT particles. It can be seen in Fig. 7b that the intensity of this peak strongly depends on the composite inorganic content. To our best knowledge, the appearance of the additional transition in the spectra of the PVDF-HFP composite has not been reported yet. For this reason, we paid a special attention to this effect. $\varepsilon''(T)$ curves of all four materials obtained at different frequencies (in the interval between 0.15 and 500 kHz) are given in Fig. 8. As can be seen in Fig. 8a, the dielectric loss curves of PVDF HFP have a single transition peak, which shifts toward higher temperature with increasing in frequency. The $\varepsilon''(T)$ curves of the

composites, in contrast, exhibit an additional peak, clearly distinguishable in the narrow frequency range from 158 Hz to ~100 kHz (the endpoints of the intervals depended slightly on the NKBT content in the composite). For example, in the sample with 10 wt% of NKBT (Fig. 8d), the mentioned peak appears at 158 Hz and it shifts towards lower temperature as frequency increases. At the frequencies of ~25 kHz, the transition can be recognized as a shoulder, while at the frequencies above 100 kHz, it merges with (in that temperature range) a more pronounced glass transition peak.

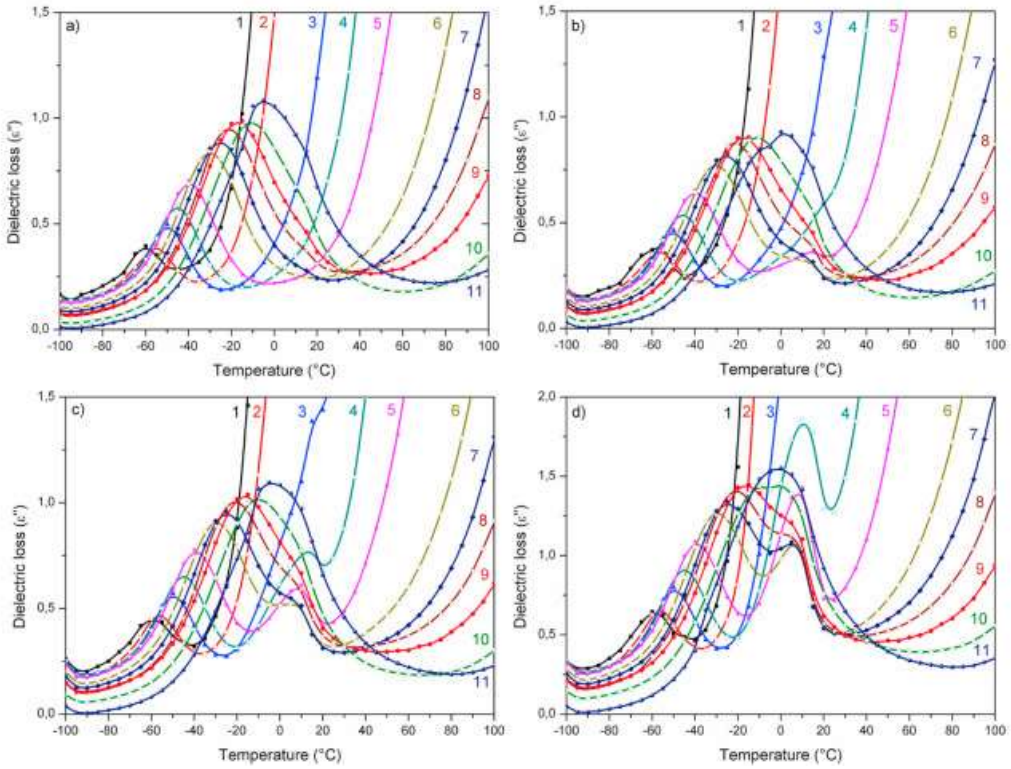

Download : Download high-res image (1MB)

Download : Download full-size image

Fig. 8. Dielectric loss versus temperature curves for the pure a) PVDF-HFP and PVDF-HFP/NKBT composites with b) 2.5, c) 5, d) 10 wt% of filler. The spectra are recorded at 1) 0,16 Hz, 2) 1 Hz, 3) 25 Hz, 4) 158 Hz, 5) 1 kHz, 6) 10 kHz, 7) 25 kHz, 8) 50 kHz, 9) 100 kHz, 10) 251 kHz, and 501 kHz.

The origin of the additional process in the ε''(T) spectra of the composites is yet to be explained. However, it should be noted that increasing the amount of the polar β-crystals by co-polymerization of VDF with HFP also resulted in the appearance of the process at higher temperature (at about 35 °C), which was not observed in the spectra of the pure PVDF [46]. It was also shown that the intensity of this particular process depends of the content of HFP co-monomer [47]. Recently, similar effect was observed in dielectric loss spectra of poly(vinylidenefluoride-trifluoroethylene-chlorofluoroethylene) (P(VDF-TrFE-CFE)) terpolymer films by Venkatesan et al. [48]. After introduction of CFE monomer, the ε''(T) spectra recorded at low constant frequencies exhibited additional transition at ~20 °C. At higher frequencies (~10^4 Hz), this peak merges with glass transition peak. The authors argue that the steric effects of the bulky chlorine atoms in the third monomer affect the crystallization process and reduce the size of ferroelectric domains to a few nanometers. For this reason, this terpolymer exhibits specific dielectric and piezoelectric properties. It is possible that the introduction of the NKBT particles induce similar effect in PVDF-HFP matrix. The segmental motions in the particle-chain interface regions will be different from the segmental motions of the chains in the bulk of the matrix (Tanaka model suggests that the size of the interfacial regions is up to tens of nanometers).

4. Conclusions

NKBT perovskite particles with R3c crystal symmetry were synthesized by sol-gel method. When used as filler, the obtained ceramic particles induce an increase in dielectric constant of PVDF-HFP matrix in the whole range of investigated frequencies (at fixed temperatures). Dielectric loss ($\varepsilon''(T)$) spectra of the composite materials exhibited the additional relaxation peak, which was not present in the spectrum of the pure co-polymer. The observed relaxation transition occurred above the glass transition temperature and its intensity (at fixed frequency) increased with increasing in amount of NKBT. This novel process is frequency dependent and it can be clearly resolved in the $\varepsilon''(T)$ spectra measured at frequencies between 160 Hz and 50 kHz. The dielectric spectra at low frequencies (0.1–10 Hz) and high temperatures (T > 70 °C) show strong increase in dielectric constant, which is attributed to conductivity relaxations.

Author statement

V.P.P. Raman and dielectric spectroscopy measurements, data analysis; D.T. data analysis, visualization, draft preparation; R.D. preparation of composite samples; D.D. dielectric spectroscopy and other electric measurements; M.D.D. and M.M. fabrication and characterization of NKBT filler; M.McP. DSC measurements, data analysis; V.B.P. Methodology and SEM measurements; B.V. and V. Dj. conceived the project and the methodology; V.Dj. Writing- Reviewing and Editing of the paper.

Data availability

The raw/processed data required to reproduce these findings cannot be shared at this time as the data also forms part of an ongoing study.

Declaration of competing interest

The authors declare that they have no known competing financial interests or personal relationships that could have appeared to influence the work reported in this paper.

Acknowledgements

The authors would like to thank Dr Amira Meddeb (Materials Research Institute, Penn State University) for her kind assistance and help during dielectric measurements. The research was funded by the Ministry of Education, Science and Technological Development of the Republic of Serbia (Project Nos. 172056, 45020 and 171029) and projects NSF CREST (HRD-0833184) and NSF (1523617).

Appendix A. Supplementary data

The following is the supplementary data related to this article:

Download : **Download Word document (621KB)**

Multimedia component 1.

Recommended articles

References

[1] Prateek, V.K. Thakur, R.K. Gupta
Recent progress on ferroelectric polymer-based nanocomposites for high energy density capacitors: synthesis, dielectric properties, and future aspects
Chem. Rev., 116 (2016), pp. 4260-4317, 10.1021/acs.chemrev.5b00495

View Record in Scopus Google Scholar

[2] M.T. Sebastian, H. Jantunen
Polymer–ceramic composites of 0–3 Connectivity for circuits in electronics: a review
Int. J. Appl. Ceram. Technol., 7 (2010), pp. 415-434, 10.1111/j.1744-7402.2009.02482.x
View Record in Scopus Google Scholar

[3] S. Ducharme
An inside-out approach to storing electrostatic energy
ACS Nano, 3 (2009), pp. 2447-2450, 10.1021/nn901078s
View Record in Scopus Google Scholar

[4] A. Jain, P. K.J., A.K. Sharma, A. Jain, R. P.N
Dielectric and piezoelectric properties of PVDF/PZT composites: a review
Polym. Eng. Sci., 55 (2015), pp. 1589-1616, 10.1002/pen.24088
View Record in Scopus Google Scholar

[5] P. Singh, H. Borkar, B.P. Singh, V.N. Singh, A. Kumar
Ferroelectric polymer-ceramic composite thick films for energy storage applications
AIP Adv., 4 (2014), p. 87117, 10.1063/1.4892961
Google Scholar

[6] R.H. Upadhyay, R.R. Deshmukh
Investigation of dielectric properties of newly prepared β-phase polyvinylidene fluoride–barium titanate nanocomposite films
J. Electrost., 71 (2013), pp. 945-950, 10.1016/j.elstat.2013.08.004
Article Download PDF View Record in Scopus Google Scholar

[7] K. Yang, X. Huang, Y. Huang, L. Xie, P. Jiang
Fluoro-polymer@$BaTiO_3$ hybrid nanoparticles prepared via RAFT polymerization: toward ferroelectric polymer nanocomposites with high dielectric constant and low dielectric loss for energy storage application
Chem. Mater., 25 (2013), pp. 2327-2338, 10.1021/cm4010486
View Record in Scopus Google Scholar

[8] S.D. Vacche, F. Oliveira, Y. Leterrier, V. Michaud, D. Damjanovic, J.-A.E. Månson
The effect of processing conditions on the morphology, thermomechanical, dielectric, and piezoelectric properties of P(VDF-TrFE)/$BaTiO_3$ composites
J. Mater. Sci., 47 (2012), pp. 4763-4774, 10.1007/s10853-012-6362-x
Google Scholar

[9] H. Rekik, Z. Ghallabi, I. Royaud, M. Arous, G. Seytre, G. Boiteux, A. Kallel
Dielectric relaxation behaviour in semi-crystalline polyvinylidene fluoride (PVDF)/TiO_2 nanocomposites
Compos. B Eng., 45 (2013), pp. 1199-1206, 10.1016/j.compositesb.2012.08.002
Article Download PDF Google Scholar

[10] V.S. Nguyen, D. Rouxel, B. Vincent, L. Badie, F.D. Dos Santos, E. Lamouroux, Y. Fort
Influence of cluster size and surface functionalization of ZnO nanoparticles on the morphology, thermomechanical and piezoelectric properties of P(VDF-TrFE) nanocomposite films
Appl. Surf. Sci., 279 (2013), pp. 204-211, 10.1016/j.apsusc.2013.04.070
Article Download PDF View Record in Scopus Google Scholar

[11] J. Dodds, F. Meyers, K. Loh
Piezoelectric nanocomposite sensors assembled using zinc oxide nanoparticles and poly(vinylidene fluoride)
Smart Struct. Syst., 12 (2013), 10.12989/sss.2013.12.1.055

Google Scholar

[12] P. Kim, S.C. Jones, P.J. Hotchkiss, J.N. Haddock, B. Kippelen, S.R. Marder, J.W. Perry
Phosphonic acid-modified barium titanate polymer nanocomposites with high permittivity and dielectric strength
Adv. Mater., 19 (2007), pp. 1001-1005, 10.1002/adma.200602422
View Record in Scopus Google Scholar

[13] P. Kim, N.M. Doss, J.P. Tillotson, P.J. Hotchkiss, M.-J. Pan, S.R. Marder, J. Li, J.P. Calame, J.W. Perry
High energy density nanocomposites based on surface-modified $BaTiO_3$ and a ferroelectric polymer
ACS Nano, 3 (2009), pp. 2581-2592, 10.1021/nn9006412
View Record in Scopus Google Scholar

[14] L. Xie, X. Huang, K. Yang, S. Li, P. Jiang
"Grafting to" route to PVDF-HFP-GMA/$BaTiO_3$ nanocomposites with high dielectric constant and high thermal conductivity for energy storage and thermal management applications
J. Mater. Chem. A., 2 (2014), pp. 5244-5251, 10.1039/C3TA15156E
View Record in Scopus Google Scholar

[15] Y. Kim, O.L. Smith, M. Kathaperumal, L.R. Johnstone, M.-J. Pan, J.W. Perry
Enhancement of breakdown strength and energy density in $BaTiO_3$/ferroelectric polymer nanocomposites via processing-induced matrix crystallinity and uniformity
RSC Adv., 4 (2014), pp. 19668-19673, 10.1039/C4RA00987H
View Record in Scopus Google Scholar

[16] Z.-M. Dang, J.-K. Yuan, S.-H. Yao, R.-J. Liao
Flexible nanodielectric materials with high permittivity for power energy storage
Adv. Mater., 25 (2013), pp. 6334-6365, 10.1002/adma.201301752
View Record in Scopus Google Scholar

[17] Y. Feng, W.L. Li, Y.F. Hou, Y. Yu, W.P. Cao, T.D. Zhang, W.D. Fei
Enhanced dielectric properties of PVDF-HFP/$BaTiO_3$-nanowire composites induced by interfacial polarization and wire-shape
J. Mater. Chem. C., 3 (2015), pp. 1250-1260, 10.1039/C4TC02183E
View Record in Scopus Google Scholar

[18] V.P. Pavlović, V.B. Pavlović, B. Vlahović, D.K. Božanić, J.D. Pajović, R. Dojčilović, V. Djoković
Structural properties of composites of polyvinylidene fluoride and mechanically activated $BaTiO_3$ particles
Phys. Scripta, T157 (2013), p. 14006, 10.1088/0031-8949/2013/t157/014006
Google Scholar

[19] T.G. Mofokeng, A.S. Luyt, V.P. Pavlović, V.B. Pavlović, D. Dudić, B. Vlahović, V. Djoković
Ferroelectric nanocomposites of polyvinylidene fluoride/polymethyl methacrylate blend and $BaTiO_3$ particles: fabrication of β-crystal polymorph rich matrix through mechanical activation of the filler
J. Appl. Phys., 115 (2014), Article 84109, 10.1063/1.4866694
Google Scholar

[20] A. Peleš, O. Aleksić, V.P. Pavlović, V. Djoković, R. Dojčilović, Z. Nikolić, F. Marinković, M. Mitrić, V. Blagojević, B. Vlahović, V.B. Pavlović
Structural and electrical properties of ferroelectric poly(vinylidene fluoride) and mechanically activated ZnO nanoparticle composite films
Phys. Scripta, 93 (2018), Article 105801, 10.1088/1402-4896/aad749
View Record in Scopus Google Scholar

[21] V.S. Nisa, S. Rajesh, K.P. Murali, V. Priyadarsini, S.N. Potty, R. Ratheesh

Preparation, characterization and dielectric properties of temperature stable $SrTiO_3$/PEEK composites for microwave substrate applications
Compos. Sci. Technol., 68 (2008), pp. 106-112, 10.1016/j.compscitech.2007.05.024
Article Download PDF View Record in Scopus Google Scholar

[22] Y. Hu, Y. Zhang, H. Liu, D. Zhou
Microwave dielectric properties of PTFE/$CaTiO_3$ polymer ceramic composites
Ceram. Int., 37 (2011), pp. 1609-1613, 10.1016/j.ceramint.2011.01.039
Article Download PDF View Record in Scopus Google Scholar

[23] L. Zhang, P. Wu, Y. Li, Z.-Y. Cheng, J. Brewer
Preparation process and dielectric properties of Ba0.5Sr0.5TiO3–P(VDF–CTFE) nanocomposites
Compos. B Eng., 56 (2014), pp. 284-289, 10.1016/j.compositesb.2013.08.029
Article Download PDF View Record in Scopus Google Scholar

[24] M. Wang, J. Zhu, W. Zhu, B. Zhu, J. Liu, X. Zhu, Y. Pu, P. Sun, Z. Zeng, X. Li, D. Yuan, S. Zhu, G. Pezzotti
The formation of percolative composites with a high dielectric constant and high conductivity
Angew. Chem. Int. Ed., 51 (2012), pp. 9123-9127, 10.1002/anie.201203389
View Record in Scopus Google Scholar

[25] D. Bhadra, A. Biswas, S. Sarkar, B. Chaudhuri, K. Tseng, H. Yang
Low loss high dielectric permittivity of polyvinylidene fluoride and $K_xTi_yNi_{1-x-y}O$ (x=0.05, y=0.02) composites
J. Appl. Phys., 107 (2010), Article 124115, 10.1063/1.3437633
View Record in Scopus Google Scholar

[26] M. Li, M. Pietrowski, R. Souza, H. Zhang, I. Reaney, S. Cook, J. Kilner, D. Sinclair
A Family of oxide ion conductors based on the ferroelectric perovskite $Na_{0.5}Bi_{0.5}TiO_3$
Nat. Mater., 13 (2014), p. 31, 10.1038/nmat3782
Google Scholar

[27] M. Veera Gajendra Babu, S.M. Abdul Kader, M. Muneeswaran, N. V Giridharan, D. Pathinettam Padiyan, B. Sundarakannan
Enhanced piezoelectric constant and remnant polarisation in K-compensated sodium potassium bismuth titanate
Mater. Lett., 146 (2015), pp. 81-83, 10.1016/j.matlet.2015.01.152
Article Download PDF View Record in Scopus Google Scholar

[28] G.A. Babu, R. Subramaniyan @ Raja, I. Bhaumik, S. Ganesamoorthy, P. Ramasamy, P.K. Gupta
Growth and characterization of undoped and Mn doped lead-free piezoelectric NBT–KBT single crystals
Mater. Res. Bull., 53 (2014), pp. 136-140, 10.1016/j.materresbull.2014.02.017
Article Download PDF View Record in Scopus Google Scholar

[29] M.V.G. Babu, B. Bagyalakshmi, L. Venkidu, B. Sundarakannan
Grain size effect on structure and electrical properties of lead-free $Na_{0.4}K_{0.1}Bi_{0.5}TiO_3$ ceramics
Ceram. Int., 43 (2017), pp. 12599-12604, 10.1016/j.ceramint.2017.06.137
Article Download PDF View Record in Scopus Google Scholar

[30] H. Yang, M. Yan, Y. Liu, C. Li, C. Wang
A novel mineralizer-facilitated, composition-controllable route to the synthesis of small cubes of bismuth sodium potassium titanate
Integrated Ferroelectrics Int. J., 144 (2013), pp. 169-175, 10.1080/10584587.2013.787858
Google Scholar

[31] H. Zhang, S. Jiang, K. Kajiyoshi

Preparation and characterization of sol–gel derived sodium–potassium bismuth titanate powders and thick films deposited by screen printing
J. Alloys Compd., 495 (2010), pp. 173-180, 10.1016/j.jallcom.2010.01.114
Article Download PDF View Record in Scopus Google Scholar

[32] R. Sun, J. Wang, F. Wang, T. Feng, F. Kong, X. Liu, Y. Li, H. Luo
Growth and electrical properties of $Na_{0.5}Bi_{0.5}TiO_3$–$K_{0.5}Bi_{0.5}TiO_3$ lead-free single crystals by the TSSG method
Ceram. Int., 42 (2016), pp. 14557-14564, 10.1016/j.ceramint.2016.06.070
Article Download PDF View Record in Scopus Google Scholar

[33] H. Xie, L. Jin, D. Shen, X. Wang, G. Shen
Morphotropic phase boundary, segregation effect and crystal growth in the NBT–KBT system
J. Cryst. Growth, 311 (2009), pp. 3626-3630, 10.1016/j.jcrysgro.2009.05.031
Article Download PDF View Record in Scopus Google Scholar

[34] M. Muneeswaran, B.C. Choi, S.H. Chang, J.H. Jung
Effect of dysprosium doping on structural and vibrational properties of lead-free $(Na_{0.7}K_{0.3})_{0.5}Bi_{0.5}TiO_3$ ferroelectric ceramics
Ceram. Int., 43 (2017), pp. 13696-13701, 10.1016/j.ceramint.2017.07.081
Article Download PDF View Record in Scopus Google Scholar

[35] T. Zhang, W. Zhang, Y. Chen, J. Yin
Third-order optical nonlinearities of lead-free $(Na_{1-x}K_x)_{0.5}Bi_{0.5}TiO_3$ thin films
Optic Commun., 281 (2008), pp. 439-443, 10.1016/j.optcom.2007.09.052
Article Download PDF View Record in Scopus Google Scholar

[36] P. Nallasamy, S. Mohan
Vibrational spectroscopic characterization of form II poly(vinylidene fluoride)
Indian J. Pure Appl. Phys., 43 (2005), pp. 821-827
http://nopr.niscair.res.in/handle/123456789/8879
View Record in Scopus Google Scholar

[37] M. Kobayashi, K. Tashiro, H. Tadokoro
Molecular vibrations of three crystal forms of poly(vinylidene fluoride)
Macromolecules, 8 (1975), pp. 158-171, 10.1021/ma60044a013
View Record in Scopus Google Scholar

[38] T. Kida, Y. Hiejima, K. Nitta
Raman spectroscopic study of high-density polyethylene during tensile deformation
Int. J. Exp. Spectrosc. Tech., 1 (2016), pp. 1-6, 10.35840/2631-505X/8501
View Record in Scopus Google Scholar

[39] D.M. Hoffman
Infrared properties of three plastic bonded explosive binders
Int. J. Polym. Anal. Char., 22 (2017), pp. 545-556, 10.1080/1023666X.2017.1343110
Article View Record in Scopus Google Scholar

[40] N.A. Nikonorova, E.B. Barmatov, D.A. Pebalk, M. V Barmatova, G. Domínguez-Espinosa, R. Diaz-Calleja, P. Pissis
Electrical properties of nanocomposites based on comb-shaped nematic polymer and silver nanoparticles
J. Phys. Chem. C, 111 (2007), pp. 8451-8458, 10.1021/jp068688a
View Record in Scopus Google Scholar

[41] E. Neagu, P. Pissis, L. Apekis
Electrical conductivity effects in polyethylene terephthalate films

J. Appl. Phys., 87 (2000), pp. 2914-2922, 10.1063/1.372277
View Record in Scopus Google Scholar

[42] A. Kremer, Friedrich, Schönhals (Eds.), Broadband Dielectric Spectroscopy (first ed.), Springer-Verlag Berlin Heidelberg (2003), 10.1007/978-3-642-56120-7
Google Scholar

[43] D. Pitsa, M.G. Danikas
Interfaces features in polymer nanocomposites: a review of proposed models
Nano, 6 (2011), pp. 497-508, 10.1142/S1793292011002949
View Record in Scopus Google Scholar

[44] D. Dudić, B. Škipina, J. Dojčilović, L. Novaković, D. Kostoski
Effects of charge trapping on the electrical conductivity of low-density polyethylene-carbon black composites
J. Appl. Polym. Sci., 121 (2011), pp. 138-143, 10.1002/app.33421
View Record in Scopus Google Scholar

[45] V. Tomer, E. Manias, C.A. Randall
High field properties and energy storage in nanocomposite dielectrics of poly(vinylidene fluoride-hexafluoropropylene)
J. Appl. Phys., 110 (2011), Article 44107, 10.1063/1.3609082
Google Scholar

[46] P. Frübing, F. Wang, M. Wegener
Relaxation processes and structural transitions in stretched films of polyvinylidene fluoride and its copolymer with hexafluoropropylene
Appl. Phys. A, 107 (2012), 10.1007/s00339-012-6838-1
Google Scholar

[47] V. V Kochervinskii, I.A. Malyshkina, G. V Markin, N.D. Gavrilova, N.P. Bessonova
Dielectric relaxation in vinylidene fluoride–hexafluoropropylene copolymers
J. Appl. Polym. Sci., 105 (2007), pp. 1101-1117, 10.1002/app.26145
Google Scholar

[48] T.R. Venkatesan, A.A. Gulyakova, P. Frübing, R. Gerhard
Electrical polarization phenomena, dielectric relaxations and structural transitions in a relaxorferroelectric terpolymer investigated with electrical probing techniques
Mater. Res. Express, 6 (2019), Article 125301, 10.1088/2053-1591/ab5352
View Record in Scopus Google Scholar

Cited by (2)

The effect of core-shell BaTiO<inf>3</inf>@SiO<inf>2</inf> on the mechanical and dielectric properties of PVDF composites
2022, Polymer-Plastics Technology and Materials

Application of fractional calculus to modeling the nonlinear behaviors of ferroelectric polymer composites: Viscoelasticity and dielectricity
2021, Membranes